Thermodynamics of Hydrogen Bonding in Polymer Blends. 3. Experimental Studies of Blends Involving Poly(4-vinylphenol)

Michael M. Coleman,* Andrew M. Lichkus, and Paul C. Painter

Department of Materials Science and Engineering, The Pennsylvania State University, University Park, Pennsylvania 16802. *Received February 4, 1988*

ABSTRACT: The application of an association model describing binary polymer blends where the components interact through the formation of hydrogen bonds has provided a theoretical basis for the calculation of the free energy changes and phase diagram of these systems. This has been described in the two prior papers of this series. In this paper we compare the theoretical calculations of the phase diagrams of a number of poly(4-vinylphenol) blends with various polyacrylates, polyacetates, and polylactones to experimental observations. The results are very encouraging.

Introduction

In the preceding two papers of this series[1,2] a theoretical basis for a description of the free energy changes and phase behavior has been presented for binary polymer blend systems involving relatively strong nonrandom specific interactions. In particular, we have concentrated on the application of an association model to systems where only one of the polymers self-associates through intermolecular hydrogen bonding. The other polymer is assumed to be unassociated but is capable of association with the first, again through intermolecular hydrogen bonding. The development of this theory, per se, was very rewarding, but we would be left with a feeling of disquiet and our efforts would inevitably be doomed to obscurity if there were no practical polymer blend examples with which to test the theory. Fortunately, there are many. In the past few years, we have performed experimental studies on a number of such polymer blend systems, and these experiments fueled the theory, which has now, in turn, led to a new focus for our experimental studies.

Our preceding studies have been largely concerned with binary blends of strongly self-associated polymer containing urethane, amide, and methacrylic acid groups with essentially unassociated polymers having ether, pyridine, and oxazoline groups.[3-6] However, in this paper we will concentrate our attention on studies of polymer blends of poly(4-vinylphenol) (PVPh) with a series of polyacrylates, for two major reasons. First, PVPh and the polyacrylates are relatively stable polymers up to temperatures of about 220 °C, unlike the polymers we have previously studied containing acid, urethane, and ether groups.[3-5] Second, a homologous series of polyacrylates is readily available, and this permits a systematic variation in the molar volume of the nonassociated polymer in the blend (an analogous series of polyethers or polypyridines is much more difficult to obtain). The theory presented in the preceding two papers predicts that the ratio of the molar volumes of the blend components is an important variable in determining phase behavior. In addition, we will revisit our previously reported infrared spectroscopic results of the PVPh blends with poly(vinyl acetate) (PVAc), ethylene-*co*-vinyl acetate copolymers (EVA),[7] and polyesters[8] and reconsider the interpretation of the data in the light of the development of our theory.

Experimental Section

The poly(4-vinylphenol) (PVPh), poly(vinyl acetate) (PVAc), ethylene-*co*-vinyl acetate copolymers (EVA[70], EVA[45], and EVA[25] containing 70, 45, and 25% vinyl acetate, respectively), poly(ϵ-caprolactone) (PCL), and poly(β-propiolactone) (PPL) employed in this study have been described previously.[7,8,10] The polyacrylates poly(methyl acrylate) (PMA), poly(ethyl acrylate) (PEA), poly(butyl acrylate) (PBA), and poly(2-ethylhexyl acrylate) (P2EHA) were purchased from Polysciences Inc. and have reported weight average molecular weights of 30 000, 70 000, 119 000 and 124 000, respectively. Poly(pentyl acrylate) (PPA), with a reported molecular weight of 415 000 was kindly supplied by Dr. David Walsh or Imperial College, London (currently employed at E. I. du Pont de Nemours and Co., Wilmington, DE).

Infrared spectra were recorded on either Digilab Models FTS-15E or FTS-60 Fourier transform infrared (FTIR) spectrometers at a resolution of 2 cm^{-1}. A minimum of 64 scans were signal averaged, and the spectra were stored on a magnetic disk system. Spectra recorded at elevated temperatures were obtained by using a SPECAC high-temperature cell mounted in the spectrometer and a Micristar heat controller. This device has a reported accuracy of ±0.1 °C. Thin films of the blends prepared for the FTIR and thermal analysis measurements were cast from 1% (w/v) tetrahydrofuran solutions onto potassium bromide windows or glass slides at room temperature. After the majority of the solvent had evaporated, the films were placed under vacuum at 110 °C for 4 h to completely remove residual solvent and then allowed to cool to room temperature. All samples were stored under vacuum in a desiccator to minimize water adsorption. Films used in this study were sufficiently thin to be within an absorbance range where the Beer-Lambert law is obeyed (<0.6 absorbance units). Thermal analysis was performed on a Perkin-Elmer 7 Series differential scanning calorimeter. A heating rate of 20 °C/min was employed with a sample size of approximately 10-15 mg. The glass transition temperature was taken as the midpoint of the change in heat capacity of the blend as a function of temperature.

Results and Discussion

Our primary goal in this paper is to illustrate how well the experimental observations of a significant number of different blends of PVPh with polymers containing acrylate, acetate, and ester groups fits the theoretical concepts and equations developed in the two preceding papers. There are a number of parameters required and a few important assumptions to be made, however, before we can calculate the free energy of mixing and the theoretical phase diagrams. These are described in a systematic manner below.

Determination of the Fraction of H-Bonded Carbonyl Groups. An infrared analysis of PVPh blends with PVAc, EVA, and polyesters has been described in detail in two previous publications, and it is not necessary to describe the infrared spectra of the analogous PVPh-polyacrylate blends, since the salient features are identical.[7,8] Quantitative analysis of the fraction of hydrogen-bonded acrylate groups was performed in the carbonyl stretching region by curve resolving the bands assigned to the "free" (non-hydrogen-bonded) and hydrogen bonded C=O vibrations at about 1735 and 1710 cm^{-1}, respectively.[9,10] In common with the previous studies of PVPh blends with polyacetates[7] and confirmed during this

*To whom correspondence should be addressed.

0024-9297/89/2222-0586$01.50/0

Table I
Curve-Fitting Results of Polyacrylate–PVPh Blends

vol fract acrylate:PVPh	mol fract PVPh	free C=O band freq, wavenumber	free C=O band width, wavenumber	free C=O band area	bonded C=O band freq, wavenumber	bonded C=O band width, wavenumber	bonded C=O band area	fraction bonded abs ratio = 1.5	fraction bonded error
				PMA					
14:86	0.8	1739	18	294	1716	30	808	0.65	0.02
30:70	0.6	1739	19	871	1716	30	1598	0.55	0.02
39:61	0.5	1738	19	752	1715	28	932	0.45	0.02
49:51	0.4	1738	19	1872	1715	28	1840	0.40	0.03
72:28	0.2	1739	18[a]	1776	1714	28[a]	712	0.21	0.09
				PEA					
17:83	0.8	1734	19	363	1709	27	824	0.60	0.01
35:65	0.6	1734	19	733	1709	27	1184	0.52	0.01
44:56	0.5	1734	19	625	1709	27	766	0.45	0.02
55:45	0.4	1738	19	586	1709	26	524	0.37	0.03
76:24	0.2	1739	19[a]	660	1714	26	335	0.25	0.06
				PBA					
22:78	0.8	1736	18	193	1709	28	363	0.56	0.03
42:58	0.6	1736	18	303	1709	28	559	0.55	0.04
53:47	0.5	1735	19	609	1710	29	896	0.50	0.03
62:38	0.4	1735	19	729	1709	28	788	0.42	0.04
82:18	0.2	1735	18	1229	1714	29	701	0.28	0.04
				PPA					
24:76	0.8	1735	18	329	1710	27	383	0.44	0.03
46:54	0.6	1735	17	888	1710	26	980	0.42	0.02
56:44	0.5	1735	17	1442	1711	26	1401	0.39	0.03
65:35	0.4	1735	17	1180	1711	26	1006	0.36	0.02
83:17	0.2	1736	17	1870	1714	30	936	0.25	0.04

[a] Fixed parameter.

study,[11] an absorptivity ratio (the ratio of the absorptivity of the band assigned to hydrogen-bonded groups to the absorptivity of the band assigned to "free" groups) of 1.5 was employed. At least 3 (maximum 10) different samples for each composition were measured and averaged. The results are summarized in Table I, which also includes an estimation of the errors involved.[11] For completeness, the results obtained previously for the PVPh–polyacetate[10] and PVPh–polyester[12] blends are reproduced in Table II.

Choice of Self-Association Model and Determination of the Equilibrium Constants for PVPh (K_2 and K_B). It is unfortunate that blends containing polyurethanes or polyacids have only very limited thermal stability and hence can be reliably studied only over a narrow temperature range, since the equilibrium constants describing self-association in polyurethanes[3] and polyacids[5] can be directly obtained from an infrared analysis in the carbonyl stretching region of these polymers in the condensed state. Conversely, in the case of PVPh, which is reasonably stable to temperatures of at least 220 °C, it is not presently possible to determine the self-association equilibrium constant(s) with any degree of certainty by using a similar procedure. The –OH (and –NH) stretching region of the infrared spectrum is not amenable to quantitative analysis of the "free" and hydrogen-bonded hydroxyl groups *in the solid state*. The "free" hydroxyl band is weak, difficult to quantify, and poorly resolved from the intense, broad hydrogen-bonded hydroxyl band. In addition, a complicated relationship exists between the absorption coefficients and frequency for the hydrogen-bonded hydroxyls.[9] How then do we obtain an estimation of the self-association equilibrium constant for PVPh? Fortunately, we can draw on the extensive studies performed on the low molecular weight analogue, phenol.

Whetsel and Lady[13] employed infrared spectroscopy to study dilute solutions of phenol in nonpolar solvents over a broad concentration range. The band due to "free" OH groups dominates in the near infrared and can be quantitatively measured. Infrared measurements of the OH

Table II
Experimental Data for PVPh Blends

vol fract	fract bonded (abs ratio = 1.5)	vol fract	fract bonded (abs ratio = 1.5)
	PVAc:PVPh		
7:93	0.69	61:39	0.34
22:78	0.65	86:14	0.16
40:60	0.53		
	EVA(70):PVPh		
11:89	0.68	71:29	0.34
31:69	0.63	91:9	0.16
52:48	0.53		
	EVA(45):PVPh		
17:83	0.52	81:19	0.27
44:56	0.42	94:6	0.16
64:36	0.38		
	PCL:PVPh		
21:79	0.63	66:34	0.42
36:64	0.60	81:19	0.30
51:49	0.49		

fundamental modes were also reported. Many association models were tested, and the first significant conclusion was that single-parameter models were inconsistent with the infrared data. These authors agreed with the conclusion of Coggeshall and Saier[14] that two equilibrium constants are required to describe phenol self-association, one describing the formation of dimers, K_2, and another describing the formation of higher multimers K_B (i.e., "chains" of hydrogen-bonded hydroxyl groups). A major assumption of the work presented here and one that we recognize could introduce significant (but consistent) errors is that we can obtain a reasonable estimate of the corresponding two equilibrium constants for PVPh from the solution measurements of Whetsel and Lady. With these reservations in mind, we extrapolated the solution values of K_2 = 2.10 L mol^{-1} and K_B = 6.68 L mol^{-1} (table 7, ref 13) to the solid state and, correcting for molar volume

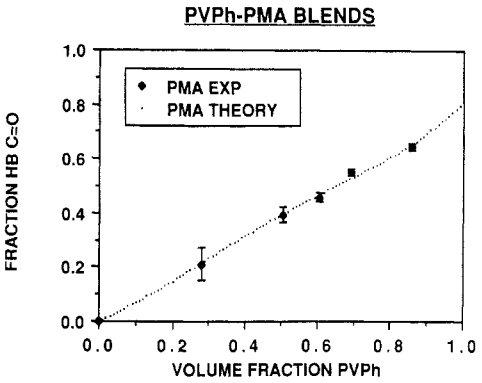

Figure 1. Comparison of the experimentally and theoretically (K_A = 53.2) determined fraction of hydrogen-bonded PMA acrylate carbonyl groups as a function of the volume fraction of PVPh.

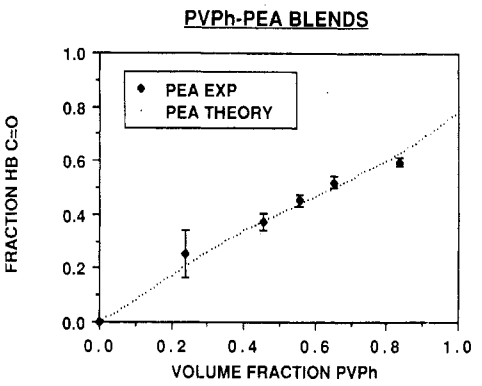

Figure 2. Comparison of the experimentally and theoretically (K_A = 46.8) determined fraction of hydrogen-bonded PEA acrylate carbonyl groups as a function of the volume fraction of PVPh.

differences as described in paper 1 of this series, calculated[11] values for PVPh of 21.6 and 68.6 for K_2 and K_B at 25 °C, respectively.

Competing Equilibria. Determination of the Association Equilibrium Constant K_A. The derivation of the equations describing the stoichiometry of binary mixtures when dimer formation in the self-associating component is described by a different equilibrium constant than the addition of each succeeding unit is presented in the Appendix of the first paper in this series.[1] The appropriate equations are

$$\Phi_B = \Phi_{B_1}\left[\left(1 - \frac{K_2}{K_B}\right) + \frac{K_2}{K_B}\left[\frac{1}{(1 - K_B\Phi_{B_1})^2}\right]\right]\left[1 + \frac{K_A\Phi_{0A}}{r}\right] \quad \text{(I)}$$

$$\Phi_A = \Phi_{0A} + K_A\Phi_{0A}\Phi_{B_1}\left[\left(1 - \frac{K_2}{K_B}\right) + \frac{K_2}{K_B}\left[\frac{1}{(1 - K_B\Phi_{B_1})}\right]\right] \quad \text{(II)}$$

where Φ_A and Φ_B are the volume fractions of non-self-associating species A and self-associating species B, respectively. Φ_{0A} and Φ_{B_1} are the volume fractions of the respective totally "free monomers", and r is the ratio of the molar volumes of the repeat units, V_A/V_B. Note that here the subscripts refer to the *chemical repeat units* and not the difficult-to-define "interacting" unit. Table III lists the values and source for all the parameters employed for the different polymers used in this study. Finally, K_A is the equilibrium constant describing the association of A with B, and it is upon the experimental determination of this constant that our attention is next focused.

PVPh–Polyacrylate Blends. The graphs in Figures 1 and 2 show the experimental values of the fraction of hydrogen-bonded acrylate carbonyl groups as a function of the volume fraction of PVPh in blends of this polymer with PMA and PEA. We have determined that these mixtures are unambiguously miscible at room temperature across the whole composition range, exhibiting a single intermediate T_g as determined by thermal analysis.[11] A similar conclusion has been reached by others for the analogous polymethacrylates.[15] Employing the values of K_2 and K_B determined above (21.6 and 68.6, respectively) and selecting an initial value for K_A together with the appropriate value of r (Table III), we calculated the roots (Φ_{B_1}) iteratively using Newton's method for given values of Φ_B over the whole composition range (eq I and II). The fraction of hydrogen-bonded acrylate groups as a function of the volume fraction of PVPh is then simply given by $1 - [\Phi_{0A}/\Phi_A]$. The value of K_A was systematically varied, and a least-squares method employed to determine the best fit of the experimental data for the PVPh blends with PMA and PEA. The theoretical curves derived from the best estimates of K_A = 53.2 and 46.8 for blends with PMA and PEA, respectively, are also illustrated in Figures 1 and 2. The splendid fit is most encouraging. All things being equal (i.e., no major changes in chemistry, steric hindrance, etc.), we theoretically predicted that identical values of K_A for similar PVPh–polyacrylate blends should be found.[1] The difference in the size of the chemical repeat units is accounted for by the factor K_A/r in the equations. Given the experimental limitations inherent in the infrared analysis, the two estimates of K_A are in remarkably good agreement. Accordingly, an average value of K_A = 50 is used in all our subsequent calculations for PVPh–polyacrylate blends.

(It might occur to the reader that an unbiased estimation of the three equilibrium constants could be obtained by permitting them all to vary in a least-squares best fit of the experimental data, thus removing the need to transfer values of K_2 and K_B from solution measurements. Unfortunately, this is not feasible as the equations are classically ill conditioned. That is, we can obtain numerous different solutions yielding acceptable best fits of the data within the limits of the experimental error. Values of the

Table III
PVPh Blends, Parameter List

polymer	V^a	$N_A{}^b$	$K_A{}^c$	δ^d	χ^e
PVPh	97.4			11.23	
PMA	70.1	350	53.2	9.88	0.300
PEA	86.6	700	46.8	9.52	0.481
PBA	119.5	1000		9.10	0.746
PPA	135.9	3000		8.97	0.840
P2EHA	185.0	700		8.56	1.173
PVAc	72.3	3000	64.0	9.56	0.459
EVA (70)	115.5	3000	61.6	8.98	0.833
EVA (45)	195.6	3000		8.58	1.155
EVA (25)	375.0	3000		8.31	1.403
PPL	57.5	3000		10.25	0.158
PCL	106.9	3000	66.2	9.21	0.671
P7L	139.8	3000		8.92	0.878
P9L	172.7	3000		8.75	1.012

parameter	value	parameter	value
N_B	60	ΔH_2, kcal/mol	5.6
K_2	21.6	ΔH_B, kcal/mol	5.2
K_B	68.6	ΔH_A, kcal/mol	4.3

[a] V is molar volume. [b] N_A is degree of polymerization. [c] K_A is equilibrium constant. [d] δ is solubility parameter. [e] χ is interaction parameter.

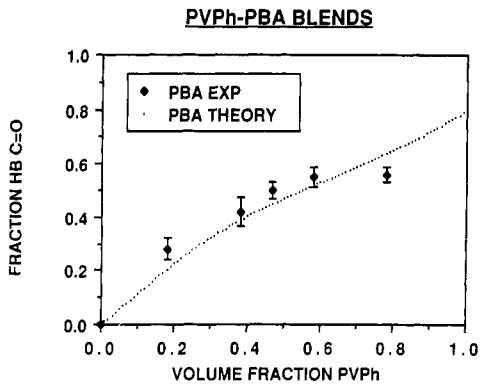

Figure 3. Comparison of the experimentally and theoretically (K_A = 50) determined fraction of hydrogen-bonded PBA acrylate carbonyl groups as a function of the volume fraction of PVPh.

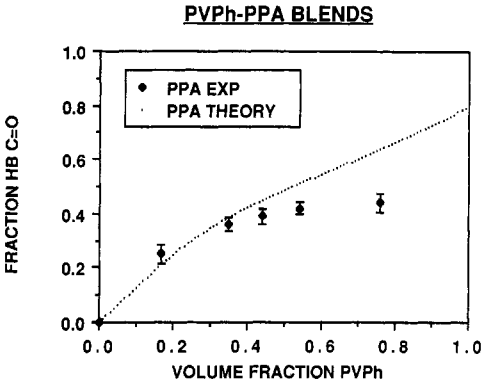

Figure 4. Comparison of the experimentally and theoretically (K_A = 50) determined fraction of hydrogen-bonded PPA acrylate carbonyl groups as a function of the volume fraction of PVPh.

self-association constants need to be independantly determined, at least in this system.)

A comparison of the theoretical curves (K_2 = 21.6, K_B = 68.6, and K_A = 50) and the experimental results for PVPh–PBA (r = 1.33) and PVPh–PPA (r = 1.40) blends is given in Figures 3 and 4. A reasonable fit of the experimental data for the former blend system is obtained by using the value of K_A = 50 derived from the miscible PVPh blends with PMA and PEA. This is consistent with the thermal analysis studies of the PVPh–PBA blends which indicate that the system is practically miscible. Distinct intermediate T_g's are observed that closely follow the Fox–Flory[16] relationship. There is, however, a suggestion of a T_g corresponding to essentially pure PVPh in blends containing high concentrations of PVPh (>80%).

In marked contrast, the fit of the experimental data to the theoretical curve (K_A = 50) for the PVPh–PPA blends is poor except in the case of the PPA-rich blends (Φ_B < 0.4). This is an important observation and can be interpreted in one of two ways. Either the model is inappropriate and the previous fits to experimental data were somewhat fortuitous, or the deviations are due to phase separation. The thermal analysis data are complex but indicate that PVPh–PPA blends are not miscible (defined as a single phase over the whole composition range). Two distinct T_g's are evident in the blends containing >50% PVPh, whereas in PPA-rich blends only a single T_g, closely corresponding to that calculated from the Fox–Flory equation, is observed. The significance of these observations will become clearer when we discuss the theoretical phase diagrams.

PVPh–Polyacetate and –Polylactone Blends. Table II lists the fraction of hydrogen-bonded acetate (or ester) groups, as determined by infrared analysis, for three different PVPh–polyacetate blends[7,10] and one PVPh–polylactone blend.[8,10,12] Blends of PVPh with PVAc, EVA[70], and PCL have been shown to be miscible in the amorphous state between room temperature and 200 °C over the entire composition range.[7,8,10,17] Using a procedure identical with that described above for the PVPh–PMA (PEA) blends (see Table III for the specific parameter values used), we determined the value of K_A by the least-squares fitting procedure of the experimental data (see Figures 5–7). Values of K_A = 64.0, 61.6, and 66.2 were determined for the PVPh blends with PVAc, EVA[70], and PCL, respectively. These values are very similar, again consistent with our theoretical predictions, and an average value of K_A = 64 is used in our subsequent calculations on all PVPh blends with polyacetates and polyesters.

PVPh–EVA[45] blends are known to be multiphased systems.[17] As in the case of the multiphased PVPh–PPA

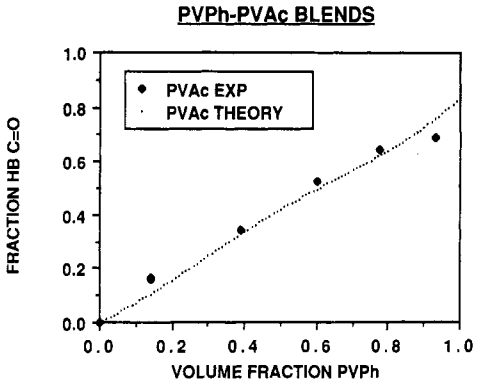

Figure 5. Comparison of the experimentally and theoretically (K_A = 64.0) determined fraction of hydrogen-bonded PVAc acetate carbonyl groups as a function of the volume fraction of PVPh.

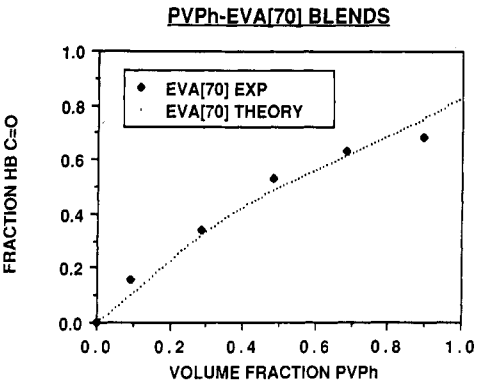

Figure 6. Comparison of the experimentally and theoretically (K_A = 61.6) determined fraction of hydrogen-bonded EVA[70] acetate carbonyl groups as a function of the volume fraction of PVPh.

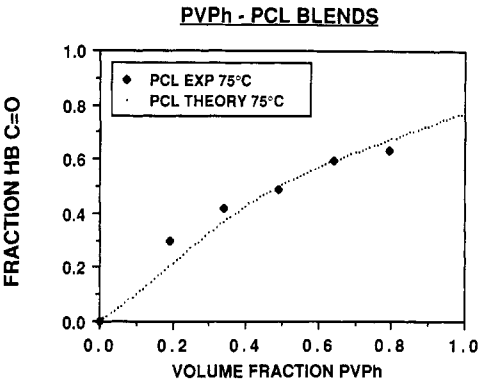

Figure 7. Comparison of the experimentally and theoretically (K_A = 66.2) determined fraction of hydrogen-bonded PCL ester carbonyl groups as a function of the volume fraction of PVPh.

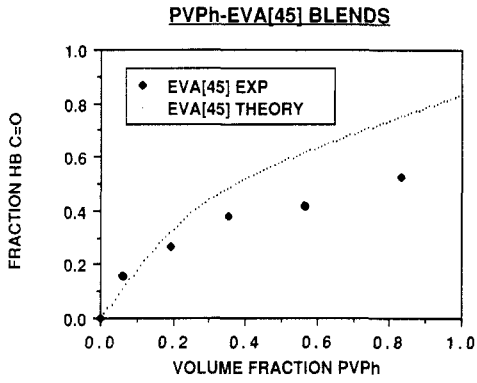

Figure 8. Comparison of the experimentally and theoretically (K_A = 64) determined fraction of hydrogen-bonded EVA[45] acetate carbonyl groups as a function of the volume fraction of PVPh.

blends described above, the theoretical curve of the fraction of hydrogen-bonded acetate carbonyls as a function of volume fraction PVPh for these blends shows poor agreement with the experimental data (see Figure 8). This is especially true for the PVPh-rich blends, and we will return to this observation later.

Calculation of the Free Energy of Mixing. Having obtained the three equilibrium constants K_2, K_B, and K_A, we are now in a position to calculate the free energy of mixing using the equations derived in the Appendix of the first paper of this series.[1] Also included in that Appendix is a detailed description of all the parameters involved. In summary, the relevant equations are

$$\frac{\Delta G^M}{RT} = \frac{\Phi_A}{N_A} \ln \Phi_A + \frac{\Phi_B}{N_B} \ln \Phi_B + \Phi_A \Phi_B \chi + \frac{\Delta G_H}{RT} \quad \text{(III)}$$

where

$$\frac{\Delta G_H}{RT} = \Phi_B \ln \left[\frac{\Phi_{B_1}}{\Phi_{B_1}^0 \Phi_B^{(1/\bar{n}_H^0)}} \right] + \frac{\Phi_A}{r} \ln \left[\frac{\Phi_{0A}}{\Phi_A} \right] + \Phi_B \left[\frac{\Gamma_1^0}{\Gamma_2^0} - \frac{\Gamma_1}{\Gamma_2} \right] + \Phi_B \left[\frac{\Gamma_1}{\Gamma_2} \right] \left[\frac{X}{1+X} \right] \quad \text{(IV)}$$

The superscript 0 denotes the parameter in the pure state and

$$\Gamma_1 = \left(1 - \frac{K_2}{K_B}\right) + \frac{K_2}{K_B}\left(\frac{1}{1 - K_B \Phi_{B_1}}\right) \quad \text{(V)}$$

$$\Gamma_2 = \left(1 - \frac{K_2}{K_B}\right) + \frac{K_2}{K_B}\left(\frac{1}{(1 - K_B \Phi_{B_1})^2}\right) \quad \text{(VI)}$$

The corresponding values of Γ_1^0 and Γ_2^0 are obtained by substituting $\Phi_{B_1}^0$ for Φ_{B_1} and

$$\bar{n}_H^0 = \Gamma_2^0 / \Gamma_1^0 \quad \text{(VII)}$$

Before calculating the free energy of mixing, we are going to need values for the molar volumes, degrees of polymerization of A and B, and the interaction parameter χ. We now consider the source and justification of the values employed for these parameters.

Molar Volumes V_A and V_B and the Degrees of Polymerization N_A and N_B. The molar volumes of the chemical repeat units for the various polymers shown in Table III were calculated from the individual group contributions listed in van Krevelen's book.[18] Unless otherwise stated, the values employed for N_A and N_B (Table III) represent realistic estimations determined by dividing the reported number-average molecular weights of the different polymers by their respective repeat unit molar masses. No attempt was made to allow for polydispersity.

Interaction Parameter χ. In most cases the value of χ is unknown and it is appropriate to regard it as an adjustable parameter. An initial estimate of χ can be obtained from solubility parameters, however, and as we shall see this gives surprisingly successful results for the systems described here. Accordingly, we define χ as follows:[19]

$$\chi = \frac{V_B}{RT}[\delta_A - \delta_B]^2$$

The solubility parameters were calculated from the molar attraction constants of Hoy.[20] The results are included in Table III.

(It might at first seem to be a gross inconsistency to include an interaction term calculated from solubility parameters, as it is well-known that this approach is valid only in the absence of specific interactions. As we pointed out in paper 1 of this series, however, for low molecular weight materials the hydrogen-bonding interactions can be treated separately and, in effect, are used to define the distribution of "chains" of molecules present. These hydrogen-bonded chains are randomly arranged relative to one another and interact through weak dispersion and other forces in the same manner as covalently linked chains of equivalent character. Our χ parameter refers to the repulsive forces between unlike segments in such chains, and we postulate that to a first approximation these physical forces can be estimated from solubility parameters. This seems most reasonable in that the hydrogen-bonding interactions have been removed from consideration and serve only to define the equilibrium distribution of species present. The only additional assumption made to those inherent in lattice models of this type is that the convalently linked polymer chains under consideration are sufficiently flexible to allow hydrogen bonds to form according to their natural proclivities.)

Room-Temperature Calculations. Employing the parameters described above in eq I–VII, we calculated the free energy of mixing as a function of the volume fraction of PVPh in various blends. The results for five PVPh–polyacrylate systems at 25 °C are displayed in Figure 9. Also included in Figure 9 are plots of the numerically determined second derivative of the free energy with respect to PVPh volume fraction. (An analytical solution was obtained for the two equilibrium constant self-association model used in this study, but is algebraically complicated. The two methods gave identical results.)

The calculated results predict that at 25 °C the PVPh blends with PMA, PEA, and PBA are miscible. The free energy of mixing is negative, and the second derivative is positive throughout the whole composition range—the definition of a miscible system. Experimentally, single intermediate T_g's have been found by thermal analysis for the PVPh–PMA and –PEA systems throughout the entire composition range.[11] For the PVPh–PBA system, while single intermediate T_g's are observed most of the composition range, there is evidence of two T_g's at high PVPh concentrations (>80%). On the other hand, the PVPh–PPA and –P2EHA blend systems are predicted to be multiphased. The free energy is not negative throughout the entire composition range and consequently the second derivative assumes negative values over a certain composition range. Experimentally, PVPh–PPA blends exhibit two distinct T_g's in blends containing >50% PVPh and no measurable fraction of hydrogen-bonded acrylate carbonyl groups was detected for the PVPh–P2EHA blend system,[11] indicating an essentially immiscible system. Incidentally, it did not escape our attention that the second

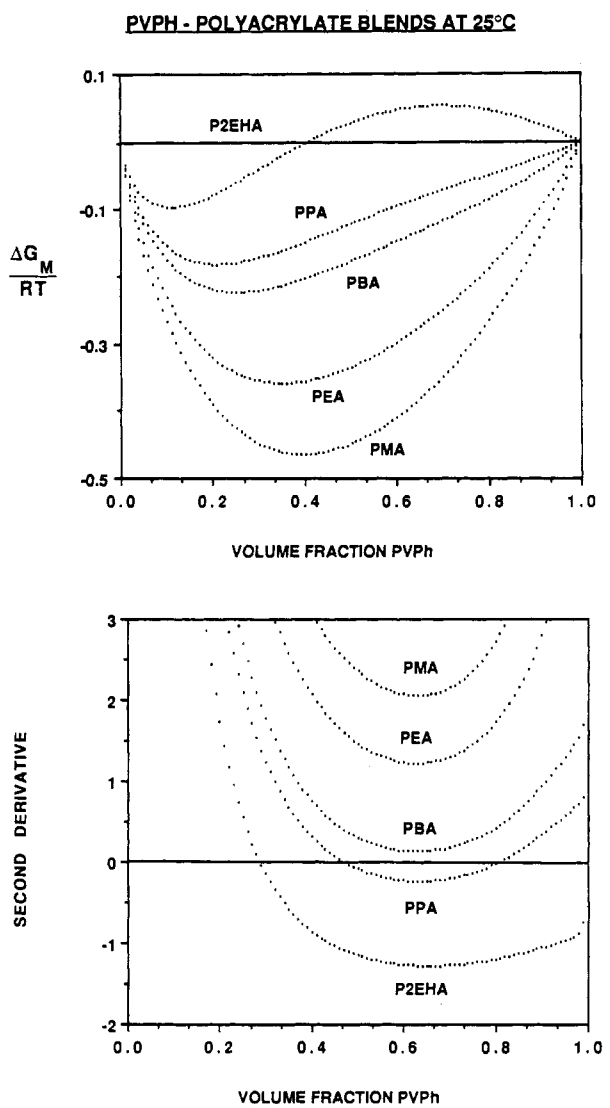

Figure 9. Calculated free energy of mixing and second derivatives of the free energy for PVPh–polyacrylate blends at 25 °C.

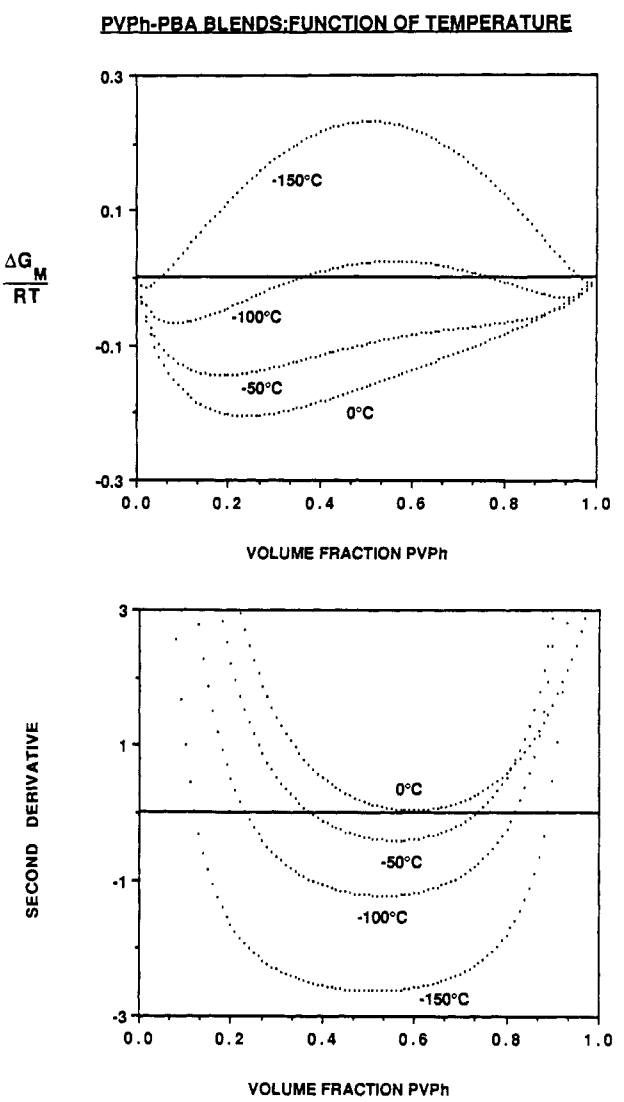

Figure 10. Calculated free energy of mixing a second derivatives of the free energy for PVPh–PBA blends at various temperature below 0 °C.

derivative curve for the PVPh blends with PBA is dangerously close to assuming a negative value at 25 °C—an encouraging observation since it suggests this system is on the margin of miscibility.

So far so good, but what we would really like is the phase diagram, or at least the spinodal, which may be readily determined by equating the second derivative to zero. For this we need to calculate the free energy as a function of temperature, which in turn requires us to make two further assumptions.

Temperature Dependence of the Equilibrium Constants and χ. Our approach to the temperature dependence of the equilibrium constants K_2, K_B, and K_A is straightforward. A van't Hoff relationship is assumed and a constant ΔH employed over the entire temperature range considered (−150 to 500 °C). [We fully recognize that ΔH will vary over such a wide temperature range but not to a significant degree judging from infrared frequency shifts of the carbonyl bands with temperature (25–220 °C) in the PVPh–polyacetate blends.[7] In addition, this is purely an equilbrium model and does not address questions such as the restricted mobility below the glass transition temperature or degradation of the polymer at elevated temperatures.] Values of the enthalpy of hydrogen bond formation of 5.6, 5.2, and 4.3 kcal mol^{-1} corresponding to the three equilibrium constants K_2, K_B, and K_A were obtained from the literature.[13,22,23]

The temperature dependence of the interaction parameter, χ, is assumed to follow a simple inverse temperature relationship in this study. More complicated relationships such as those outlined by Patterson and co-workers[25] can be incorporated at a later date, if necessary.

Effect of Temperature on Free Energy. To demonstrate the effect of temperature on the free energy of mixing and the second derivative thereof, we have used PVPh–PBA blends as an example because as we have seen (Figure 9) this system is on the margin of miscibility at room temperature. Calculations were performed over a temperature range of −150 to 200 °C by using the parameters listed in Table III and the results are depicted in Figures 10 and 11. At −150 °C the free energy is positive and the second derivative negative over the vast majority of the composition range. Between about −90 and 0 °C the free energy is everywhere negative. Only at 0 °C is the second derivative everywhere positive, however, ensuring miscibility at this temperature over the entire composition range. From 0 to 200 °C the free energy is always negative. Nonetheless, the second derivative is not everywhere positive above about 90 °C. Consequently, there is a "window" or range of compositions over which the system is multiphased, defined by the compositions at which the second derivative is zero, which in this system is biased toward the PVPh-rich blends. These points, of course, define the spinodal.

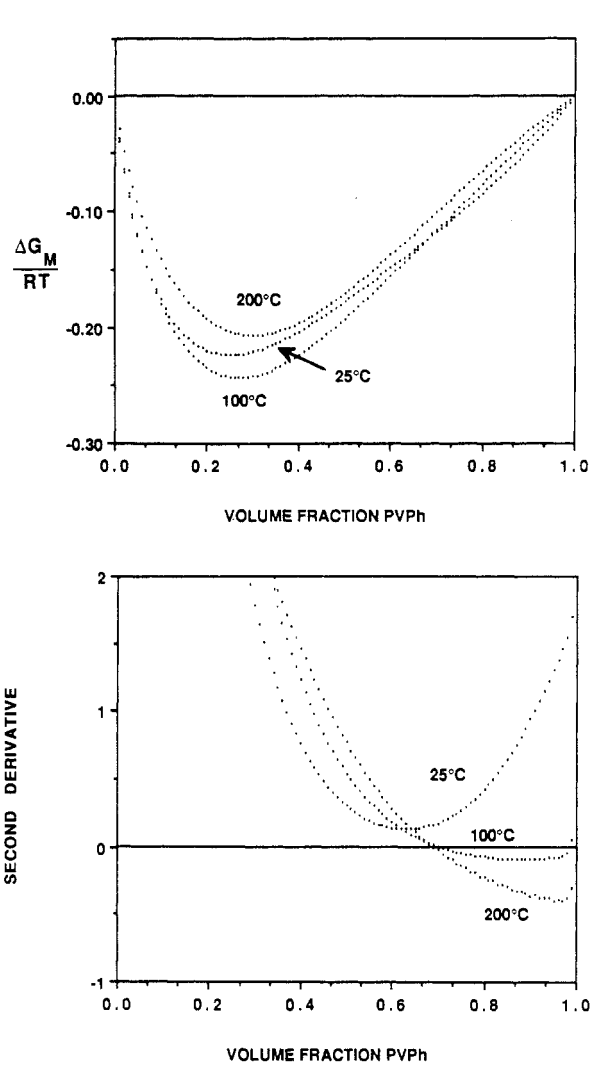

Figure 11. Calculated free energy of mixing and second derivatives of the free energy for PVPh–PBA blends at various temperatures above 25 °C.

Calculation of the Phase Diagram. Generalizing the method for determining the spinodal described immediately above, we calculated the phase diagram for a number of PVPh blend systems. We first consider the blends with polyacrylates.

PVPh–Polyacrylate Blends. Figure 12 shows the calculated phase diagrams for PVPh blends with PBA, PPA, and P2EHA. The corresponding phase diagrams for the PMA and PEA blends yielded no spinodal information over the temperature range considered. This infers that these systems are *theoretically* completely miscible over a temperature range of −100 to 500 °C. Experimentally, the PVPh blend systems with PMA and PEA are miscible at least from room temperature to 200 °C.[11]

The phase diagram calculated for the PVPh–PBA blends is at first glance extraordinary but nevertheless typical of hydrogen bonded systems.[1] The presence of a closed loop spinodal, which defines an "area of immiscibility" in the phase diagram, *hypothetically* permits a PVPh-rich blend which is immiscible at very low temperatures to pass through a region of miscibility into a phase-separated zone and finally once again become miscible as the temperature is elevated—a classic reappearing phase behavior. It should be noted that a "window" of miscibility extends throughout the entire composition range (between 0 and 90 °C). In addition, for

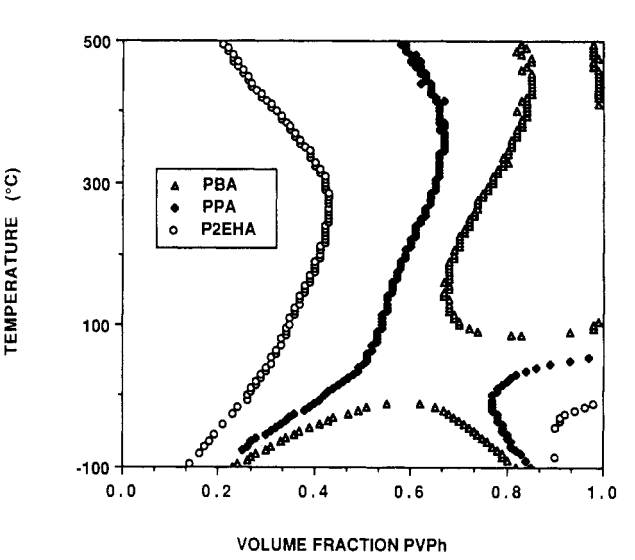

Figure 12. Calculated spinodals for PVPh–polyacrylate blends.

Table IV
PVPh–PPA Blends: Thermal Analysis Results

blend	T_{g1}	T_{g2}	T_g(Fox–Flory)
100:0	140		140
80:20	140	−10	73
60:40	143	−7	25
50:50	140	−12	5
20:80		−37	−40
0:100		−63	−63

PVPh-rich blends the calculations predict phase separation into pure PVPh and an enriched PPA phase at temperatures above about 90 °C. The calculations also predict that for compositions of less than 65% PVPh no spinodal decomposition will occur, at least throughout the temperature range of 0 to 500 °C. Again, experimentally the PVPh–PBA system appears essentially miscible, but as mentioned previously, there is evidence for a second phase in PVPh-rich blends.[11]

(A note of caution is warranted concerning the extent of the composition range over which the system is phase separated. The binodal, which describes the limits of metastability, exceeds the boundary of the spinodal. The calculation of the binodal is not trivial. Nevertheless, a numerical estimation of the binodal can be calculated by searching for equivalent chemical potentials outside the spinodal consistent with a common tangent to the free energy curve. We are writing a computer program to do just this.)

The spinodal phase diagram calculated for the PVPh–PPA blends predicts phase separation for PVPh-rich blends throughout the entire temperature range considered. In contrast, PPA-rich blends are predicted to be single-phased materials over the same temperature range. In light of these results, an examination of the thermal analysis data for the PVPh–PPA system presented in Table IV is germane. Let us first consider a PVPh-rich blend (say 80% PVPh). It is predicted that this blend should separate into an essentially pure PVPh phase and a correspondingly lean (about 50%) PVPh–PPA mixture. Significantly, PVPh-rich blends do exhibit two T_g's, one corresponding to pure PVPh (140 °C) and the other a very broad transition occurring at approximately −10 °C (Table IV). The latter temperature corresponds to a 42:58 PVPh–PPA blend based on the Fox–Flory equation and so is in general agreement with our theoretical prediction. In addition, the PPA-rich blends exhibit a single inter-

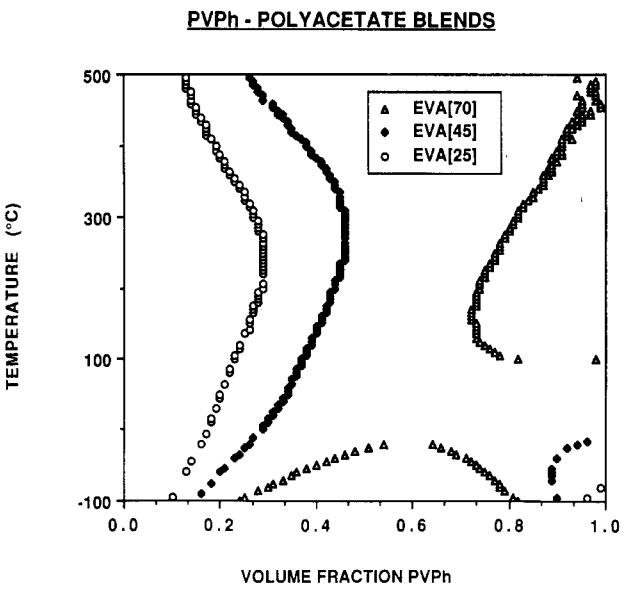

Figure 13. Calculated spinodals for PVPh–polyacetate blends.

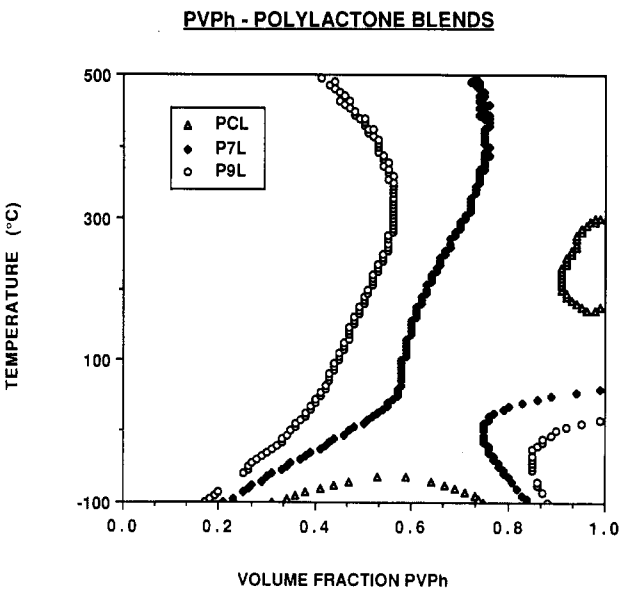

Figure 14. Calculated spinodals for PVPh–polylactone blends.

mediate T_g close to that predicted by using the Fox–Flory equation. Finally, an experimentally determined cloud point curve has been reported by other workers for this system and a minimum was reported at 120 °C for a 50:50 wt% PVPh–PPA blend.[21]

The spinodal diagram pertaining to the PVPh–P2EHA blends shows the typical "hour glass" spinodal consistent with an immiscible blend system. Only at the edges of the composition range are there regions where the two polymers are predicted to mix at the molecular level. Experimentally, the PVPh–P2EHA system is indeed an immiscible blend.

To summarize these results, the model we have employed to describe the phase behavior of PVPh–polyacrylates is in broad general conformity with the experimental results.

PVPh–Polyacrylate and –Polylactone Blends. Figures 13 and 14 show the calculated spinodal phase diagrams for PVPh blends with a series of polyacetates and polylactones, respectively. The corresponding phase diagrams for the PVAc and PPL are not shown since our calculations yielded no spinodal information over the temperature range considered. This infers that these systems are *theoretically* miscible over a temperature range of at least −100 to 500 °C. (Obviously, our model does not take into account the possibility of crystallinity, degradation, and/or kinetic effects.) For the PVPh–EVA[70] and PVPh–PCL systems an upper phase boundary is calculated and there is a closed loop region of immisciblity starting above 100 °C in blends rich in PVPh content (>70%). To all intent and purposes these systems are *theoretically* miscible above about −20 °C up to at least 500 °C over the greater part of the composition range. Experimentally, the PVPh blend systems with PVAc, EVA[70], PPL, and PCL are miscible from at least room temperature (or above T_m in the case of the latter two polymers) to 200 °C,[17] in good agreement with these predictions.

The calculated spinodals for the PVPh blends with EVA[45], EVA[25], P7L (a hypothetical polylactone containing seven methylene groups), and P9L (nine methylene groups) are of similar "hourglass" appearance, differing only in degree but not in kind. For the PVPh–EVA[25] system, the classic hourglass phase diagram characteristic of a practically immiscible system is consistent with the FTIR results that indicated the presence of only a very small fraction of hydrogen-bonded acetate groups.[7] In the case of the EVA[45] blend, however, there is a considerable portion of the phase diagram where the blend is predicted to be single phased (PVPh content <40%). This is consistent with the overall conclusion reached in our previous thermal studies that PVPh–EVA[45] blends are "intermediate multiphased systems".[17] In effect, a PVPh-rich blend again separates into an essentially pure PVPh phase and a mixed phase of intermediate composition lean in PVPh. This results in a *reduced* number of hydrogen-bonded acetate groups in PVPh–EVA[45] blends vis-à-vis the corresponding miscible PVAc and EVA[70] blends (see Figure 8, ref 7). This also explains why the theoretical curve of the fraction of hydrogen bonded acetate carbonyls as a function of volume fraction PVPh deviates from the experimental data for these blends (Figure 8). Finally, our calculations predict similar "intermediate multiphased systems" for the polylactones containing seven to nine methylene groups and it would be an interesting test of the validity of our model to obtain these polyesters and experimentally determine the phase behavior of these blends.

A "Question of Balance". The calculated phase diagrams presented in this paper may be considered as a natural progression from one in which there exists only a single inverted "U-shaped" phase boundary (type I, e.g., the miscible PVPh blends with PMA, PEA, PVAc, and PPL), to those exhibiting two distinct regions consisting of this inverted U-shaped boundary plus a "closed-loop" region (type II, e.g., the PVPh blends with PBA, PCL, and EVA[70]), to finally an hourglass phase diagram formed from the merging of the two regions (type III, e.g., the PVPh blends with PPA, P2EHA, EVA[45], EVA[25], P7L, and P9L). Categorizing the phase diagrams into these three major types is convenient for the forthcoming discussion.

It is important to show for systems predicted to exhibit type I and III phase diagrams that modest changes to the values of the parameters employed in the calculations will not significantly affect the outcome. This is readily understood if one considers the overall balance of eq III. Consider a case where both polymers have high molecular weights (the combinatorial entropy terms are thus negligible), then the free energy of mixing is determined by the balance between the $\Phi_A\Phi_B\chi$ and hydrogen-bonding terms. If the latter should *dominate* then a phase diagram of type

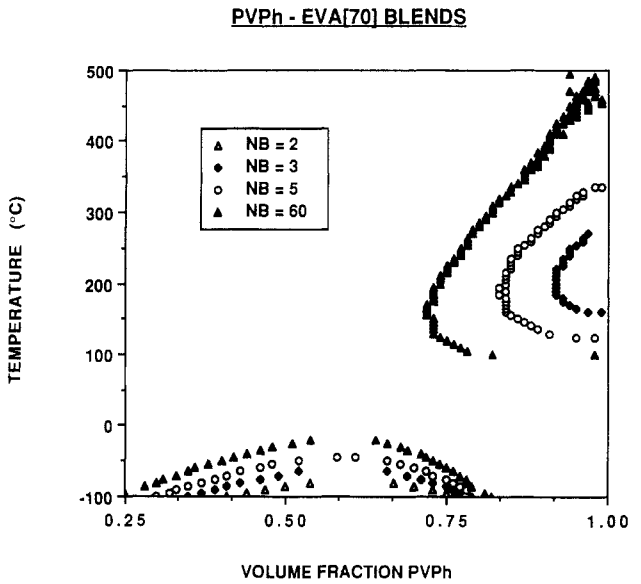

Figure 15. Calculated spinodals for PVPh–EVA[70] blends as a function of PVPh degree of polymerization.

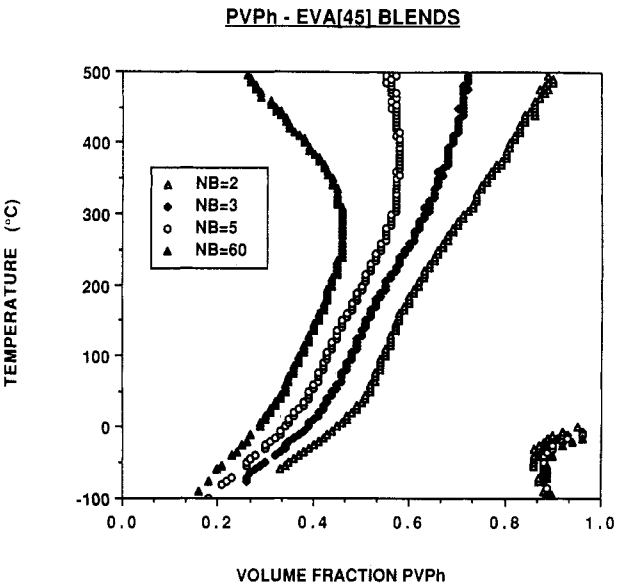

Figure 16. Calculated spinodals for PVPh–EVA[45] blends as a function of PVPh degree of polymerization.

I will result. This would remain true even if we include a dependence of χ on free volume (usually small for two polymers). Conversely, a phase diagram of type III will result should the $\Phi_A\Phi_B\chi$ term *dominate*. Where it becomes very interesting is in the transition between type II and type III phase diagrams when these two major contributors roughly balance. Now changes in molecular weight, equilibrium constants, interaction parameter, etc. can significantly alter the appearance of the phase diagram and change the limits of the "windows of miscibility". We will illustrate this by calculating hypothetical phase diagrams of PVPh–EVA blends as a function of molecular weight.

Figures 15 and 16 show calculated phase diagrams (see Table III for parameters employed) for the PVPh–EVA-[70] and-–EVA[45] systems with a constant value for the polyacetate degree of polymerization N_A = 3000 and varying the degree of polymerization for PVPh from N_B = 2 to 60. Starting with the EVA[70] blends, for the PVPh dimer (N_B = 2) the phase diagram is of type I and the system is predicted to be completely miscible at temperatures above −75 °C. For the PVPh trimer (N_B = 3) we calculate a beautiful example of the type II phase diagram. A closed-loop region extending from about 150 to 250 °C at high PVPh concentrations is predicted and yields a miscibility window throughout the composition range between −50 and 150 °C. Between N_B = 5 through N_B = 60, both the inverted U-shaped and closed-loop regions enlarge and reach a limit where increasing N_B further makes little difference. Turning our attention now to the EVA[45] blends, we see that even at N_B = 2 there is a merging of the inverted U-shaped and the closed-loop regions, resulting in a large two-phase area skewed toward high PVPh compositions. With increasing PVPh degree of polymerization, the phase diagram takes on the form of the classical hourglass (type III).

The above predictions have a direct bearing on the results recently published concerning the effect of cross-linking on the degree of molecular mixing in phenolic–EVA[70] mixtures, in which we concluded, from a quantitative analysis of the fraction of hydrogen-bonded acetate groups, that phase separation occurred upon cross-linking.[25] Our model predicts that when an oligomeric phenolic resin is polymerized (by chain extension, branching, and cross-linking reactions) in the presence of an EVA[70] polymer, phase separation should take place. Furthermore, perhaps we can begin to answer the questions posed in the concluding remarks of ref 25, since there are a number of important implications arising from the theoretical calculations of the phase diagrams. For example, since the PVPh blends with PMA and PVAc have phase diagrams of type I, this implies that the hydrogen-bonding contribution dominates the free energy of mixing and a truly miscible semiinterpretating network should now be possible.

Acknowledgment. We gratefully acknowledge the support of the National Science Foundation, Polymers Program, and the donors of the Petroleum Research Fund, administered by the American Chemical Society. A.M.L. acknowledges the support of the South African Council for Scientific and Industrial Research.

Registry No. PVPh, 24979-70-2; PMA, 9003-21-8; PEA, 9003-32-1; PBA, 9003-49-0; PPA, 37017-37-1; PVAc, 9003-20-7; EVA, 24937-78-8; PCL (homopolymer), 24980-41-4; PCL, 25248-42-4; P2EHA, 9003-77-4.

References and Notes

(1) Painter, P. C.; Park, Y.; Coleman, M. M. *Macromolecules*, first of a series of three papers in this issue.
(2) Painter, P. C.; Park, Y.; Coleman, M. M. *Macromolecules* second of a series of three papers in this issue.
(3) Coleman, M. M.; Skrovanek, D. J.; Hu, J.; Painter, P. C. *Macromolecules* **1988**, *21*, 59.
(4) Skrovanek, D. J.; Coleman, M. M. *Polym. Eng. Sci.* **1987**, *27*, 857.
(5) Lee, J. Y.; Painter, P. C.; Coleman, M. M. *Macromolecules* **1988**, *21*, 346; **1988**, *21*, 954.
(6) Lichkus, A. M.; Painter, P. C.; Coleman, M. M. *Macromolecules*, in press.
(7) Moskala, E. J.; Howe, S. E.; Painter, P. C.; Coleman, M. M. *Macromolecules* **1984**, *17*, 1671.
(8) Moskala, E. J.; Varnell, D. F.; Coleman, M. M. *Polymer* **1985**, *26*, 228.
(9) Skrovanek, D. J.; Painter, P. C.; Coleman, M. M. *Macromolecules* **1986**, *19*, 699.
(10) Moskala, E. J. Ph.D. Thesis, The Pennsylvania State University, 1984.
(11) Lichkus, A. M. Ph.D. Thesis, The Pennsylvania State University, 1988.
(12) Howe, S. E. Ph.D. Thesis, The Pennsylvania State University, 1985.
(13) Whetsel, K. B.; Lady, J. H. In *Spectrometry of Fuels*; Friedel, H., Ed.; Plenum: London, 1970; p 259.
(14) Coggeshall, N. D.; Saier, E. L. *J. Am. Chem. Soc.* **1951**, *73*, 5414.
(15) Goh, S. H.; Siow, K. S. *Polym. Bull.* **1987**, *17*, 453.

(16) Fox, T. G. *Bull. Am. Phys. Soc.* **1952**, *2*, 493.
(17) Moskala, E. J.; Runt, J. P.; Coleman, M. M. Advances in Chemistry Series, No. 211, *Multicomponent Polymer Materials*, Paul, D. R., Sperling, L. H., Eds.; American Chemical Society: Washington, D. C.; Chapter 5, 1986.
(18) van Krevelen, P. W. *Properties of Polymers*; Elsevier: Amsterdam, 1972.
(19) Kraus, S. *J. Macromol. Sci., Rev. Macromol. Chem.* **1972**, *C7*-(2), 251.
(20) Hoy, K. L. *J. Paint Technol.* **1970**, *42*, 76.
(21) Fruitwala, H. M.S. Thesis, Imperial College, London, 1985.
(22) Neerinck, D.; van Audenhaege, A.; Lamberts, L. *Ann. Chim.* **1969**, *4*, 43.
(23) Sellier, G.; Wojtkowiak, B. *J. Chim. Phys. Physicochim. Biol.* **1968**, *65*(5), 936.
(24) Biros, J.; Zeman, L.; Patterson, D. *Macromolecules* **1971**, *4*, 30.
(25) Coleman, M. M.; Serman, C. J.; Painter, P. C. *Macromolecules* **1987**, *20*, 226.

High-Resolution Images of Defects in Liquid-Crystalline Polymers: Image Analysis Using Light Diffractometer and Computer Techniques

I. G. Voigt-Martin,* H. Durst, and H. Krug

Institut für Physikalische Chemie, Johannes Gutenberg Universität, Jakob-Welder Weg 15, D-6500 Mainz, West Germany. *Received May 3, 1988; Revised Manuscript Received August 8, 1988*

ABSTRACT: In an earlier paper, electron microscope images of smectic planes and lattice planes in liquid-crystalline polymers in smectic and crystalline phases were shown for the first time. Lattice defects in the form of edge dislocations were observed in both cases. The precise nature of the dislocation core and the planes in apparently disordered regions was not uniquely determined because of the poor signal/noise ratio. In this paper, two techniques of image reconstruction are demonstrated: light diffractometry and computer analysis. In both cases, considerably improved images are obtained. The analysis of defects is critically examined.

Introduction

Using high-resolution techniques, it has been possible to directly image the smectic planes in liquid-crystal (LC) polymers and the lattice planes in a crystalline LC polymer.[1-4] More important, it has been possible to demonstrate unambiguously the presence of edge dislocations in both systems.[5] At the same time, the structure of smectic planes in liquid crystals was shown to differ from lattice planes in crystalline LC polymers by the undulations which were always observed even in otherwise perfect regions. However, a few problems remain in the image analysis from the original micrographs, and they are inherent in the method of high-resolution imaging in low-contrast objects, namely the low signal/noise ratio. This problem becomes particularly aggravating in those regions where orientation is not perfect and in the regions close to the dislocation core.

There are two different approaches to this problem; both of them are very time consuming, but the improvement in image quality is very convincing. The first method involves the use of a light diffractometer and the second a computer. In this work, both techniques have been used, and the results are compared for identical locations on the specimen.

Image Reconstruction Using a Light Diffractometer

The method of image reconstruction using a light diffractometer is not new. It was used to obtain improved images of the tobacco mosaic virus in a classical paper by Klug and de Rosier[6] and is based on the methods discussed in books on optical transforms.[7] This technique, using a light diffractometer, involves two stages of transformation: the first from real space (the electron micrograph, which is the object) to reciprocal space (the Fourier transform of the electron micrograph) and back to real space (the Fourier transform of the intensity distribution in reciprocal space, which is the image). The diffraction pattern includes the Fourier frequencies from the desired structure, such as the smectic planes, as well as those from the background noise. By allowing only those spatial frequencies obtained from the smectic planes to pass through an aperture situated in the reciprocal plane, the noise can be filtered out of the micrograph. An example of such a procedure is shown in Figure 1. It is clear that the filtered image is a considerable improvement over the unfiltered one with regard to the signal/noise (S/N) ratio. However, with the aid of Figure 2, showing the diffraction pattern obtained by light diffractometry of the micrograph in Figure 1a, it is convenient to demonstrate some technical difficulties: The sharp maxima in the light diffractogram arise from the smectic planes, while the "amorphous" halo is produced by the noise in the electron micrograph. The radius of the halo depends on the precise value of defocus which was used in obtaining the original electron micrograph. This influences the electron microscope phase contrast transfer function $\sin \chi(k)$, where k is the wave vector and

$$\chi(k) = \frac{2\pi}{\lambda}\left[-\frac{1}{4}C_s k^4 + \frac{1}{2}\Delta f k^2\right]$$

C_s is the spherical abberation constant and Δf the defocus value. In high-resolution imaging, one normally adjusts electron microscope defocus, Δf, so that the structure maxima coincide with the first minimum of the transfer function. The desired spatial frequencies can then be selected without any disturbing noise. However, in high-resolution imaging of beam-sensitive samples, the electron microscope has to be adjusted before exposing the sample to the beam, so that such a precisely defined defocus cannot normally be achieved. Inspection of Figure 2 shows that there is a weak second maximum in the $\sin^2 \chi(k)$ function near the second-order reflection from the smectic planes. However, because $\sin \chi(k)$ has passed through zero, this second reflection is transferred with contrast opposite to that of the first and would, in fact, adversely affect the

0024-9297/89/2222-0595$01.50/0